Effect of Polymer−Particle Interaction in Swelling Dynamics of Ultrathin Nanocomposite Films

2 AUTHORS:

Amarjeet Singh
Himachal Pradesh University
15 PUBLICATIONS **262** CITATIONS

SEE PROFILE

Manabendra Mukherjee
Saha Institute of Nuclear Physics
98 PUBLICATIONS **874** CITATIONS

SEE PROFILE

Effect of Polymer−Particle Interaction in Swelling Dynamics of Ultrathin Nanocomposite Films

Amarjeet Singh and M. Mukherjee*

Surface Physics Division, Saha Institute of Nuclear Physics, 1/AF, Bidhannagar, Kolkata 700064, India

ABSTRACT: The studies of solvent mass uptake and swelling dynamics of CdS−polyacrylamide nanocomposite ultrathin films in saturated solvent (H_2O) vapor were carried out. The nanocomposite material was synthesized via a chemical route. The films were prepared by spin-coating on silicon substrates. The mass uptake behavior of solvent molecules into the films, studied using the gravimetric method, was found to be film thickness dependent and of non-Fickian in nature. The swelling dynamics was studied using X-ray reflectivity as a function of swelling time. As a result of the polymer nanoparticle interaction, the dynamical behaviors of mass uptake and swelling for the nanocomposite films were observed to be widely different from our earlier observation for the pure polymer films. A mathematical model was proposed to describe the swelling behavior of the nanocomposite films in terms of the combination of a fraction of polymer molecules with somewhat restricted freedom of movement and the ones that are free. About 5−9% chains were found to have restricted motion to describe the swelling of the nanocomposite films which was close to the volume fraction of the CdS particles in the composite. The dynamical constants for the swelling of the restricted chains were found to be orders of magnitude different than those of the free chains.

1. Introduction

When a dry bulk polymer is exposed to a solvent, the solvent molecules enter into the porous structure of the polymer and diffuse into all accessible volume. If the polymer is soluble in the solvent, there is a strong attractive interaction between the polymer and the solvent and the net interaction between the polymer segments is repulsive. As a result, the coiled polymer chains start to swell as soon as they are in contact with the solvent molecules. In other words, the polymer starts to go into the solvent as it is in the early stage of the solvation process. Eventually this process would lead to a complete solution of the polymer provided there is enough solvent. The dynamics of polymer chains near surfaces and interfaces for ultrathin polymer films in the presence of solvent are of technological importance in many areas like emulsion, coating, and adhesion but have not been studied until recently.[1,2]

The dispersion of nanometer-sized inorganic particles in polymer matrix offers a new class of materials known as organic−inorganic nanocomposite materials or hybrid nanocomposite materials. Only a small amount of dispersed inorganic phase may drastically modify the physical properties of the organic matrices.[3,4] Therefore, a range of activities have been generated with such materials.[5−7] One of the most extensively studied nano-crystalline material is CdS due to their tunable optical properties.[8−10] The optical band gap of the CdS nano-particles can be tuned by manipulating the size of the crystallites and can be used as solar devises for energy conversion[11] and other applications.[12,13] In a recent publication we have discussed the novel structural aspects of spin-coated films prepared from CdS−poly-acrylamide nanocomposite material.[3] The thicknesses of the films were found to occur only in some allowed thickness range rather than changing continuously with the spin-coating speed. The observed discreteness in the film thickness was due to the presence of discrete number of layers of composite polymer coils in their structure. The effect of modification in the internal structure of the nanocomposite films as compared to the pure polymer ones are likely to be reflected in their dynamical behavior. This motivates us to carry out the present investigation.

In the present article, we discuss the role of dispersed inorganic nanoparticles on the mass uptake and swelling dynamics of nanocomposite ultrathin films. We have performed X-ray reflectivity and gravimetric measurements to study the dynamical behavior of the swelling as a result of solvent uptake for ultrathin CdS−polyacrylamide nanocomposite films supported on silicon substrates. The mass uptake studies were carried out using the gravimetric technique. The diffusion of water vapor in the nanocomposite films was observed to be non-Fickian in nature. The polymer chains are more constrained to be aligned along the substrate in the thinner films, and as a result the accessibility of the available free volume becomes restricted for the water molecules, resulting in the slower diffusion of water vapor in thinner films. The diffusion of the nanocomposite in the presence of water vapor, or in other words swelling of the films, was studied by observing the changes in the film thickness using the X-ray reflectivity technique. The swelling dynamics of the composite films were not in agreement with the free chain swelling model discussed in our earlier publication.[1] It was necessary to modify the model for the inclusion of the effect of polymer particle interaction. A fraction of polymer chains that are directly attached to the nanoparticles lose the freedom of motion and hence demonstrate different dynamical behavior than that of the free chains.

2. Experimental Section

2.1. Sample Preparation. The nanocomposite was chemically synthesized by dispersing the CdS nanoparticles in polyacrylmide matrix. To prepare the material with the CdS

concentration of 5 vol %, a measured amount of cadmium acetate was dissolved in 0.2 mg/mL of polyacrylamide ($M_w = 5 \times 10^6$, BDH Chemicals, U.K.) solution in Millipore water. 500 mL of above solution was kept boiling at 100 °C while H_2S gas was passed through the solution until the reaction was completed. It was confirmed from FTIR that H_2S gas only converts cadmium acetate into CdS and does not react with the polymer. The concentration of the final sol used for all the measurements and thin film preparation was 5.6 mg/mL. The average size of the CdS particles formed in the reaction was estimated to be 4.2 nm from the blue shift of the absorption band edge[14] measured by UV–vis spectroscopy (Cintra 10_e, GBC). Dynamic light scattering (DLS-7000, Otsuka Electronics), which measures the statistically averaged size of the polymer coils in solutions, was used to measure the hydrodynamic radius R_H of the polymer and the nanocomposite coils in solutions of above-mentioned concentrations. In this method the Stokes–Einstein equation[15] $R_H = k_B T/6\pi\eta D$ is used to obtain R_H in terms of the diffusion coefficient D of the Brownian motion of the individual polymer coils in the solution and coefficient of viscosity η of the solvent. The hydrodynamic radius for the polymer and the composite coils were found to be 1170 and 270 nm, respectively. The drastically lower R_H value for the composite coils suggests that the swelling ability of the polymer chains was reduced when they were loaded with CdS particles. This is possibly due to the fact that the different parts of a polymer chain are linked through CdS particles, and subsequent reduction in available hydrogen-bonding sites thus reduces interaction with surrounding water molecules. The nanocrystalline CdS particles are formed in the water solution in the presence of the polymer chains, and during their growth the particles are getting attached to the chains. This clearly shows that the CdS particles are attracted by the polymer molecules. Centrifugation of the composite sol at 20 000 rpm does not separate the CdS particles from the polymer chains which further suggest that the particles are preferentially attached to the polymer chains compared to the water molecules. The composite sol was used to prepare thin films on silicon (100) substrate using spin-coating technique with different rotation speeds from 500 to 5000 rpm. To make the surface suitably hydrophilic for coating of water-soluble polymers, the silicon wafers were chemically treated with a mixture of ammonia solution and hydrogen peroxide (NH_4OH: H_2O_2:$H_2O = 1$:1:2) at boiling temperature for 5 min before spin-coating on them. During the spinning, clean and warm air (60 °C) was flown gently over the sol using a homemade arrangement to facilitate a faster evaporation of water. The nominal thicknesses of the films were found in the discrete ranges of 100–155, 225–250, and 310–365 Å only. The volume fraction of the CdS particles was found to vary due to the different inter particle separation[3] as a result of stretching of the films during their preparation at different spinning speeds and was observed to be 2.7–5.0 vol %. Further details about the synthesis and various characterizations of the nanocomposite material and the thin films using transmission electron microscopy and X-ray reflectivity can be found in our earlier publication.[3] It is generally observed that the spin-coated films with high speed remain in nonequilibrium structure. The films were kept for 30 min in a closed container at saturated vapor pressure at room temperature. Since the polymer was water-soluble, the films absorbed water vapor to swell, and as a result the strain was released and the films attained equilibrium structures. The preswelled films were then stored in a desiccator for drying.

2.2. Gravimetric Measurements. The phenomenon of diffusion of solvent into the polymer, commonly known as sorption or mass uptake,[16–18] was studied using gravimetric techniques. The moisture transport in polymer systems is dependent on the availability of molecular size pores in the polymeric materials and the polymer–water affinity. The availability of the pores depends on the polymer microstructure, morphology, and degree of cross-linking.[19,20] To study the mass uptake of the films, we have used a microbalance (Metler, MT5) of microgram mass resolution. First each specimen was inserted in the closed weighing chamber and the weight of dry

composite film was recorded. Thereafter, a source of water was placed inside the chamber, and the weight of the film was recorded as a function of time. The experiment was repeated for a second time for all the samples to test the repeatability of the data. It was observed that the clean substrate also absorbs some amount of moisture initially. The data for clean substrate were subtracted from the film data to find the actual mass uptake of the composite films. The mass uptake behavior shows a release of mass after attaining the maximum in some of the films. We believe this is due to the fact that the capillary free volume would enlarge with the expansion of the film into larger pores and the water that was adsorbed purely due to the surface force would release, resulting in a weight loss in these films.

2.3. X-ray Reflectivity. X-ray reflectivity is a well-established technique to characterize the structure and morphology of surfaces and interfaces of thin films.[21,22] The nondestructive method allows one to measure the electron density of the films along their depth. The mathematical background based on electromagnetic theories initially developed by Parratt needs to approximate the films as a stack of multiple homogeneous layers with infinitely sharp buried interfaces. However, the systems like nanocomposites, in which an inorganic phase is dispersed in polymer medium, may no longer be approximated to be homogeneous. The requirement of handling these systems demands that a finite roughness of the interfaces be incorporated in the treatment.[22] In this technique, the reflectivity $R(q_z)$ is measured in reciprocal space as a function of wave vector transfer q_z which is parallel to surface normal. The Parratt formalism[23] with an appropriate modification to include the effect of surface and interfacial roughness is used to analyze the reflectivity data. In this formalism the reflectivity $R(q_z) = r_0 r_0^*$, as a function of momentum transfer q_z, is defined in an iterative scheme in terms of reflectance.

$$r_{n-1,n} = \frac{r_{n,n+1} + F_{n-1,n}}{r_{n,n+1}F_{n-1,n} + 1}\exp\left(-i\frac{4\pi}{\lambda}f_{n-1}d_{n-1}\right) \qquad (1)$$

where the Fresnel reflectance for the interface between nth and $(n-1)$th layer is modified to include the roughness σ_n of the nth layer as

$$F_{n-1,n}\frac{f_{n-1}-f_n}{f_{n-1}+f_n}\exp(0.5q_{z,n}q_{z,n-1}\sigma_n^{\,2})$$

with

$$f_n = \frac{\lambda}{4\pi}\left(q_z^{\,2} - q_{z,c}^{\,2}(n) - i\frac{8\pi\mu_n}{\lambda}\right)$$

The parameters d_n, μ_n, and $q_{z,c}(n)$ are the thickness, absorption coefficient, and critical wave vector corresponding to the nth layer, respectively. Since the reflectivity is expressed as the modulus square of the Fourier transform of the electron density ρ_e ($= 711q_{z,c}^{\,2}$ for $\lambda = 1.54$ Å), the phase information is lost, and the calculation of electron density from $R(q_z)$ is not possible. In general, the electron density variation in a specimen is determined by assuming a model for the same and comparing the calculated reflectivity profile with the experimental data. The subjectivity associated with the assumption of a model can be minimized by collecting the independent pieces of information from other experimental sources.[24] The data are analyzed using a fit program on computers. The fit program minimizes the deviations between the calculated and the observed reflectivity profiles.

In the present experiment an Enraf Nonius FR591 rotating anode generator followed by Si(111) monochromator was used as the source of Cu $K\alpha_1$ radiation. X-ray reflectivity data were collected using a Micro-control triple-axis goniometer keeping the incident and the exit angle identical for specular condition. For the swelling study the composite films were mounted in a homemade chamber equipped with two capton windows for entrance and exit of the X-ray beams. The films were first
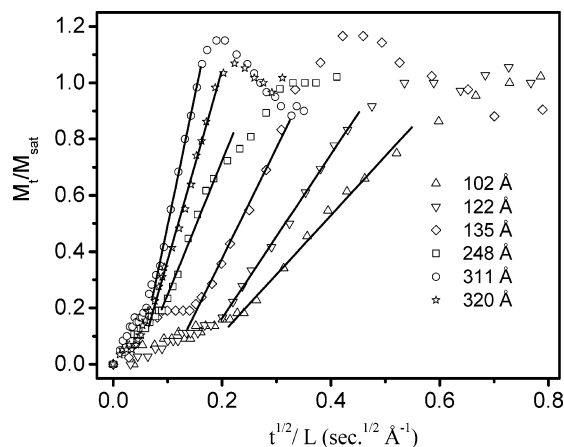
Figure 1. Normalized mass uptake against square root of time scaled with film initial thickness L. The initial thicknesses of the films are shown against the symbols. Solid lines represent the linear fits to the data.

Figure 2. Diffusion coefficient of the solvent (H_2O) as a function of film initial thickness (102, 122, 135, 248, 311, 320 Å). The dotted line shows the diffusion coefficient of water in pure polymer (from ref 1).

heated in situ up to 70 °C in a vacuum (0.07 Torr) for half an hour to expel the moisture and then cooled to room temperature before the measurements. First the X-ray reflectivity data of the dry film were taken at room temperature in a vacuum. The chamber was then opened, and a water bath was inserted in the chamber to have saturated H_2O vapor inside. The films start to swell when they are exposed to the solvent vapor. The film thickness was continuously monitored as a function of exposure time using X-ray reflectivity. The q_z range for data collection at the initial stage was carefully optimized for the data acquisition time as well as to accommodate sufficient number of thickness oscillations. Reasonably good statistics were obtained in 7−9 min for different films, during which the data were collected for each thickness. As the swelling becomes slower at the later stage, the data acquisition time and the q_z range were accordingly adjusted. When the films are completely swelled, a data with a large q_z range was taken for all the films. Data for a particular film that was not preswelled was taken for the three successive dry to swelled cycles to study the effect of residual strain on the swelling dynamics. The data were analyzed with Parratt formalism modified to include interfacial roughness as described above. The input electron density profiles were divided into layers of fixed thicknesses with an adjustable electron density and interfacial roughness to account for the presence of the CdS particles. The maximum interfacial roughness allowed was one-fourth the thickness of the corresponding layers.

3. Results and Discussion

3.1. Diffusion of Water Vapor. In our earlier study[1] with polyacrylamide thin films we observed that the process governing the diffusion of water molecule was Fickian; however, for the present case of nanocomposite films we observe non-Fickian solvent diffusion as has been observed in many polymeric systems.[2,25,26] In Figure 1 normalized mass uptake (M_t/M_{sat}) is plotted against $t^{1/2}/L$ for different films, where M_t is the mass uptake at time t defined as $M_t = (w_t - w_0)/w_0$, with w_t and w_0 denoting the weight of the film at time t and the initial weight, respectively. M_{sat} represents the saturated mass uptake. It is clearly observed from Figure 1 that the curves corresponding to the films of different thicknesses L do not coincide, indicating thickness-dependent diffusion contrary to the Fickian process. In other words, the process governing the diffusion of solvent into the nanocomposite films was non-Fickain in nature. A notable feature for all the films was the lower slope and nonlinear nature of the M_t/M_{sat} values at the initial stage of the mass uptake followed by a
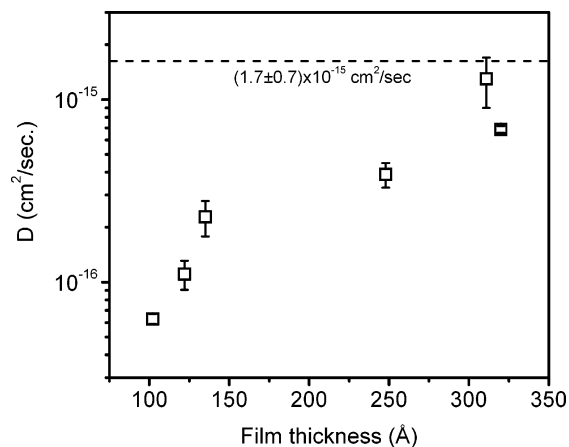
linear behavior with a higher slope. One can clearly observe from Figure 1 that the behavior of different curves in the nonlinear region extends up to about 0.2 of normalized mass uptake value and does not show any systematic pattern with change of thickness. We believe that the behavior of the curves at the initial time may be due to some nonequilibrium phenomena at the early stage of the mass uptake. The initial slower diffusion of the water molecules into the nanocomposite films may be explained in terms of the fact that the pores at the surface of the dry films are initially closed, and they open up slowly when the films are in contact with the water vapor. The opening of the surface pores are likely to be influenced by the surface properties such as roughness or morphology of a particular film, which may explain the absence of systematics in this regime. This also explains the nonlinearity of the curves in this part. Another important feature of the mass uptake behavior is the loss of weight of the films at larger time. The loss is found to be more prominent for the thicker films compared to the thinner ones. With the swelling of the films, the capillary pores that are responsible for attracting water molecules also swell, and as a result the capillarity or the attractive force would reduce; therefore, the water molecules adsorbed purely due to the surface force would leave the surface, resulting in a weight loss of the films.[1] Although the films goes on absorbing water for a longer time, the increase of the weight of the films cannot be observed as they are submerged under this weight loss phenomena at the larger time regime.

The linear behavior of the mass uptake extends between 0.2 and 0.8 of the normalized uptake values for all the curves which then bend toward abscissa. We have used the slope of the linear region of the mass uptake data to calculate the diffusion coefficient D of the water molecules into the composite films. For this purpose we have assumed the Fickian diffusion formula, $M_t/M_{sat} = (4/L)(Dt/\pi)^{1/2}$ to be valid for the linear region of the mass uptake. The use of the Fickian equation to predict the diffusion coefficients quite correctly for non-Fickian diffusions is available in the literature.[2,26,27] The diffusion coefficient was calculated for two sets of data separately for all the films, and average values as a function of initial thickness are plotted in Figure 2. It can be clearly observed that the diffusion coefficient systematically increases with the film thickness and

approaches the value close to the one observed earlier for the pure polymer[1] as shown by the dotted line in Figure 2, indicating that the diffusion behavior of water molecules in thicker nanocomposite films may be similar to that observed earlier for pure polymer films. A similar but more drastic confinement effect on diffusion coefficient was observed earlier,[2] where the effect was explained in terms of restricted diffusion of polymer chains due to confinement. However, in the present case thickness-dependent diffusion of polymer chains during swelling is not observed (discussed in the next section), and we explain the reduction of diffusion coefficient with film thickness during mass uptake in terms of the thickness-dependent structural changes in these films. With lowering of thickness of the films, the composite polymer chains are aligned in the two dimensions;[3] as a result of this ordering and the enhanced intrachain entanglement due to the attached CdS particles, the diffusing channels for the water molecules may become narrower in diameter and shorter in length, making diffusion of water difficult in thinner films. The more prominent weight loss for the thicker films compared to the thinner ones also supports the fact that for thicker films the pores are somewhat random and three-dimensional in nature and hence are more easily accessible. Once the water molecules are present in the capillary pores, they start to swell into larger pores resulting in weight loss of the films. For thinner films the pores are more restricted to the two dimensions and relatively more difficult to access; hence, the swelling of the pores and resulting weight loss is also less pronounced in these films.

3.2. Thin Film Swelling. The thicknesses of the dry nanocomposite films occur in three discrete thickness bands separated by two forbidden regions.[3] It was shown that the composite films are formed by the stacking of one or more layers of CdS loaded polymer coils that give rise to alternate low- and high-density layers along the depth of the films. The X-ray reflectivity measurements of selected films covering all the three allowed thickness regions were performed to study the swelling behavior. The scans for the dry and the completely swelled samples were taken up to a large incident angle ($q_z^{max} = 0.5$ Å^{-1}), and the scans for the intermediate swelling stages were quickly acquired up to $q_z^{max} \sim 0.1$ Å^{-1}. The reflectivity data with larger q_z^{max} range provide better special resolution; therefore, we have devised the following scheme to analyze the swelling data that are acquired up to low incident angles. First, the reflectivity data with larger q_z^{max} range (dry and completely swelled) are fit. The derived electron density profiles (EDP) were then used as the limits for the analysis of the intermediate scans. In this analysis scheme we have assumed that two successive electron density profiles would not differ very much except in the thickness. The fitted EDP corresponding to the completely swelled scan was used as input EDP for the next data and was followed for the successive data until the dry EDP was reached. The equilibrium swelling for the nanocomposite films, defined as $(t_s - t_i)/t_s$ with t_s and t_i as completely swelled and initial thicknesses, of all the films irrespective of their thicknesses was found to be 0.6 ± 0.06, which was close to the value 0.63 ± 0.04 obtained for polyacrylamide films. The reflectivity profiles of a nanocomposite film in dry and completely swelled stage are shown in Figure 3 (top panel). The corresponding electron density profiles are
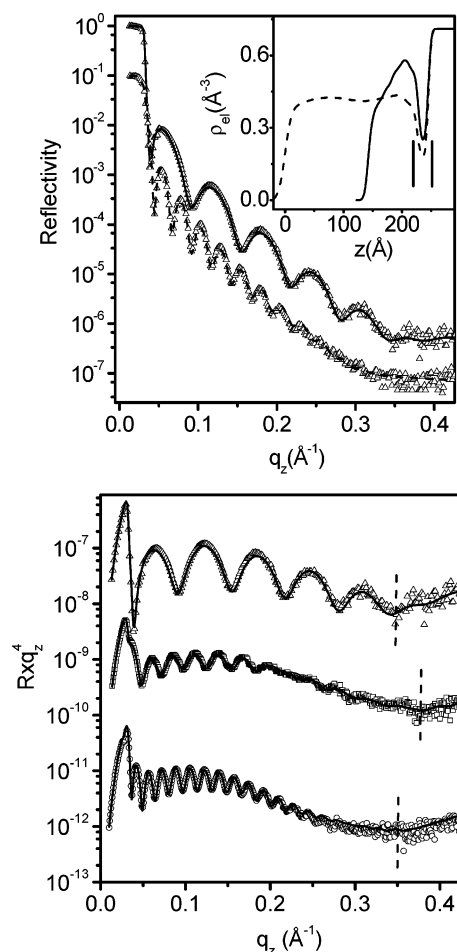
Figure 3. Top panel: X-ray reflectivity data (symbols) along with the fitted profiles (lines) of dry (102 Å) and fully swelled (244 Å) nanocomposite film. The reflectivity profile for fully swelled film is shifted downward by a decade. The inset shows the corresponding electron density profiles (ρ_{el}). The electron density profile of the dry film is shifted to right by 142 Å to match the film/substrate interface. The anchoring region near interface is marked by two parallel vertical lines. Bottom panel: plots of Rq_z^4 vs q_z for dry films of thicknesses 102 Å (up-triangle), 248 Å (square), and 363 Å (circle) with fitted profiles as lines. The dashed vertical lines represent the start of background counts.

shown in the inset of the figure. The EDP corresponding to the dry film is appropriately shifted to the right so that the polymer/substrate interfaces of both dry and swelled EDP coincide. The humplike EDP due to the presence of CdS particles in the dry stage (solid line in the inset) becomes almost uniform in the completely swelled stage (dotted line in the inset). To obtain satisfactory fitting of the X-ray reflectivity data, it was required to divide the films into slabs or layers of different electron density and interfacial roughness. A thin layer (15−18 Å) with low electron density was observed at film/substrate interface for all the nanocomposite films. For all the films the electron density of this interfacial layer was observed to be much lower than the electron density of the rest of the film. Subtle features in the reflectivity profiles can be more clearly observed if reflectivity multiplied by q_z^4 is plotted against q_z instead of reflectivity alone. In Figure 3 (bottom panel) we have shown the Rq_z^4 vs q_z for three representative films to indicate that the low-density layers close to the substrate are the true features. Two separate periodicities can be observed in the reflectivity
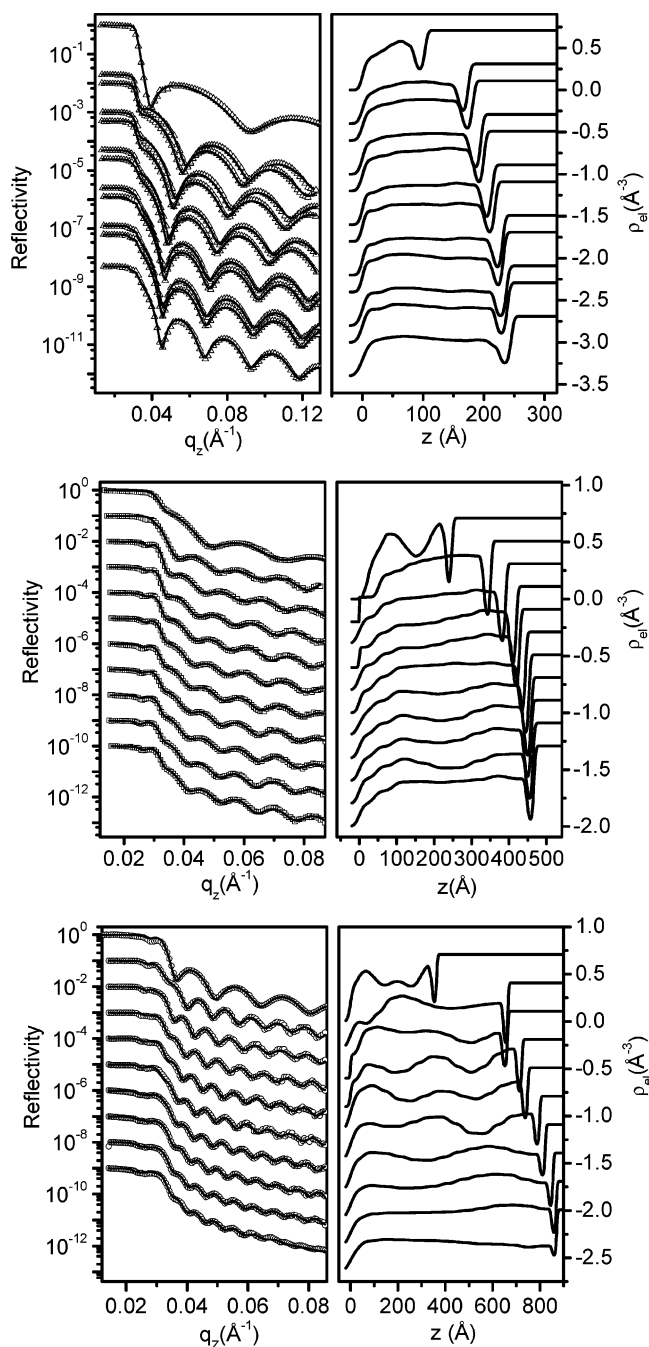
Figure 4. Left panels: X-ray reflectivity data (symbols) with fitted profiles (lines) of swelling nanocomposite films of initial thickness 102 Å (up-triangle), 248 Å (square), and 363 Å (circle). The top profile in each panel corresponds to the dry film. The profiles for swelled films are shifted downward with increasing swelling time. Right panels: electron density profiles (ρ_{el}) obtained from the fitting of the corresponding X-ray reflectivity data.

profiles in Figure 3 where the small periods corresponding to the total thickness of the films are riding on a larger period. The thickness corresponding to the large period was calculated using the relation $d \sim 2\pi/\Delta q_z$, where Δq_z is the periodicity in the reciprocal space. The obtained values of d were 15−19 Å for all the films which support the findings of the thin low-density layer at the film/substrate interface obtained from fittings. The lower value of electron density at the film/substrate interface represents the characteristic anchoring density of polymer chains.

The X-ray reflectivity data for the swelling of three nanocomposite films of widely different thicknesses (102, 248, 363 Å) taken from the three discrete thickness bands are shown in Figure 4. In the left panels in each section (top, middle, and bottom) of the figure, the reflectivity data (symbols) along with the fitted profiles (solid line) are shown. The observed EDPs are shown in the corresponding right panels. The first profiles from the top in each panel represent the dry state of the films. The profiles corresponding to the increasing swelling time are shifted downward. The nature of successive electron density profiles in top panel (102 Å) indicates that the nonuniform nature of the EDP slowly become uniform. The humplike higher electron density regions appear due to the presence of the CdS particles. The random diffusion of polymer segments on swelling almost uniformly disperses the attached CdS particles along the film thickness. In middle and bottom panels (248, 363 Å) it can be observed that initial few swelled profiles are some what different from the dry profiles. During the data acquisition time (7−9 min), several fast evolving profiles overlap, since the swelling is very fast in the beginning. Therefore, one or two initial EDPs may not represent the true physical picture. The hump structures in the EDP are found to be broader and shallower with swelling. In nanocomposite films, the number of humps in the dry EDP is equal to the number of layers of composite units stacked vertically on the substrate.[3] The observation of swelled profiles indicates that the each layer swell independently. The interdiffusion of the individual layers on swelling was ruled out since the same numbers of humps reappear in the EDPs when the films were dried again. A careful observation of the EDPs for all the swelled films indicates that only at the initial stage of the solvent exposure there was a drop of electron density at the anchoring region that remains nearly unchanged during the entire swelling process. The much lower electron density of this region ($\sim$0.2 Å^{-3}) compared to that of pure water (0.32 Å^{-3}) indicates that, contrary to the earlier observations,[28,29] the water molecules in the nanocomposite films are not accumulated at the film/substrate interface. This may be attributed to the much higher hydrophilicity of the water-soluble polymer compared to the substrate[26] used in this case.

3.3. Dynamics of the Restricted Chains. The diffusion of the polymer chains during swelling or thermal motion of the thin polymer films coated on substrates is observed to occur only along the direction perpendicular to the substrate due to the physical restriction in the other two in-plane dimensions.[1,30,31] As discussed in our earlier publication,[1] for the analysis of the swelling dynamics of thin polymer films the end-to-end distance $R(t)$ of a single free chain at time t in one dimension is described with the initial condition $R(t=0) = R_0$ as[1,32]

$$R(t) = e^{-(2D/N)t}\left[R_0{}^3 + \frac{vN^3}{2}(e^{(6D/N)t} - 1)\right]^{1/3} \qquad (2)$$

where D is the diffusion coefficient of the polymer chains, N is the degree of polymerization, and v is the excluded-volume parameter which is a positive quantity for swelling and determines the saturated thickness of the films. When the polymer film thickness is less than R_g, it is generally assumed that the films are constructed from side by side placement of a single layer

of individual polymer coils that are flattened by substrate interaction.[33] It is assumed that in the presence of solvent each individual macromolecule swells independently. Although the polymer chains are not truly free as they are mutually entangled and also bonded to the substrate, the above equation represent the swelling dynamics of the polymer films very accurately since the strong hydrophilic interactions between the solvent and the polymer molecules dominates the swelling dynamics.

In the present nanocomposite material the polymer chains are loaded with attached CdS particles, and the films are formed by the single or multiple layers of such coils.[3] We consider that the assumption of swelling of the individual coils is valid for the nanocomposite films. Because of the polymer−particle attachment, overall free movements of the polymer segments are restricted; hence, the dynamics of the polymer segments that are directly attached to the particles are likely to be different from the free polymer segments. Considering this view, we model the nanocomposite system as a sum of two components consisting of (i) a fraction of polymer segments that are directly attached to the particles and (ii) the rest of chains that are free. Assuming the dynamics of the two components to be independent, we have modified eq 2 for the description of the dynamics of a "free" and a "restricted" fraction of chains in the composite. According to this formalism, the end-to-end distance $R(t)$ of a composite polymer chain is given by

$$R(t) = R_f(t) + R_r(t) \qquad (3)$$

where

$$R_f(t) = e^{-(2D_f/N)t}\left[R_f{}^3 + \frac{v_f N^3}{2}(e^{(6D_f/N)t} - 1)\right]^{1/3}$$

and

$$R_r(t) = e^{-(2D_r/N)t}\left[R_r{}^3 + \frac{v_r N^3}{2}(e^{(6D_r/N)t} - 1)\right]^{1/3}$$

Here $R_f(t)$ and $R_r(t)$ represent the swelling of free and restricted polymer chains, respectively. D_f and D_r are respective diffusion coefficients for free and restricted parts. N is the degree of polymerization. The excluded-volume parameters for the two components v_f and v_r represent the repulsive interaction responsible for the swelling. R_f and R_r are the initial thicknesses for the free and the attached coils, respectively.

In Figure 5 we have shown the swelling behavior of the three nanocomposite films that are discussed in Figure 4. In Figure 5 we have plotted the observed thicknesses of the films as a function of swelling time along with the best fit curves obtained using eq 3. This can be clearly observed from Figure 5 that the restricted chain model described by eq 3 is in excellent agreement with the experimental data. The fit corresponding to the free chain model (eq 2) shown by the dotted lines in Figure 5 does not agree well, indicating that the swelling behaviors of the nanocomposite films are different from those of the pure polymers and cannot be treated on the same footing. The excluded-volume parameters and the diffusion coefficients of the free and the restricted parts of the nanocomposite were floating parameters for the fitting. The parameters R_f and R_r
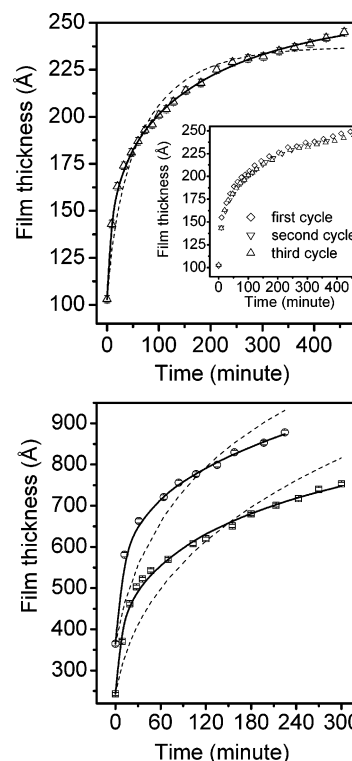
Figure 5. Thickness of the nanocomposite films as functions of swelling time. Initial thickness: 102 Å (up-triangles), 248 Å (square), and 363 Å (circle). Symbols, experimental data; dashed line, best fit eq 2; solid line, best fit eq 3. Inset in the upper panel shows three successive cycles of swelling of the thinnest film (102 Å).
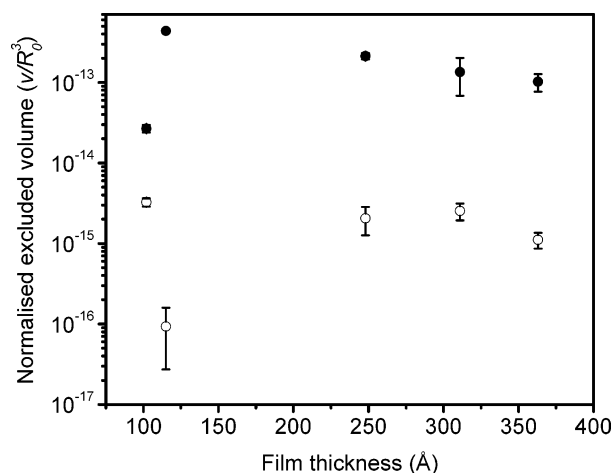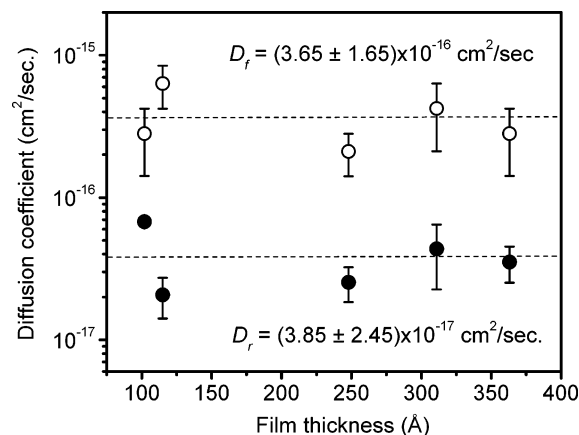

Figure 6. The normalized excluded-volume parameters for the free chain fraction v_f (open symbol) and the restricted chain fraction v_r (solid symbol) of the nanocomposite as a function of the initial film thickness (102, 115, 248, 311, and 363 Å).

were also allowed to vary within the condition that the total initial thickness $R_0 = R_f + R_r$ remains fixed.

In Figure 6 we have shown the behavior of the excluded-volume parameters corresponding to the free and the restricted sections as functions of film thickness. The parameters are plotted after normalization with dividing them by the cube of the corresponding film thicknesses. The repulsive excluded-volume interaction responsible for the swelling may be represented as $v = (1 - 2\chi)a^3$, where a^3 represents the monomer volume. The Flory interaction parameter χ may be represented as $\chi = \chi_{MS} - 1/2(\chi_{MM} + \chi_{SS})$, where the subscripts MS, MM, and SS denote the monomer−solvent, monomer−

Figure 7. Diffusion coefficients for the free chain fraction D_f (open symbol) and the restricted chain fraction D_r (solid symbol) of the nanocomposite as a function of the initial film thickness (102, 115, 248, 311, and 363 Å).

monomer, and solvent−solvent interactions, respectively.[15,33] In Figure 6 we can clearly observe that the normalized excluded-volume parameters corresponding to the restricted part of the chains are about 2 orders of magnitude larger than those corresponding to the free components. This can be understood from the fact that due to the attachment of the polymer chains via the CdS particles the monomer−monomer component of the interaction is enhanced, resulting in an enhancement of the overall excluded-volume parameter for the fraction of chains that are attached to the CdS particles. This is further supported by our observation from dynamic light scattering that the hydrodynamic radius of the CdS loaded coils are much smaller than those of the pure polymer.

The values of the diffusion coefficients for the two components D_f and D_r as obtained from the fitting of the swelling data to eq 3 are plotted in Figure 7. It can be observed that the diffusion coefficients of both free and restricted fractions are independent of the initial film thickness. The average diffusion coefficient of the "restricted" polymer fraction, $D_r = (3.85 \pm 2.45) \times 10^{-17}$ cm²/s, was almost an order of magnitude smaller than the average diffusion coefficient of the "free" polymer fraction, $D_f = (3.65 \pm 1.65) \times 10^{-16}$ cm²/s. This may be understood from the fact that due to polymer−particle interaction the freedom of the movements of the attached polymer segments is relatively more restricted compared to those of the free segments. In other words, the polymer−particle interaction slows down the dynamics of the attached segments. The observed fraction R_r of the restricted component was found to vary between 5% and 9% of the total film thickness, which was close to the volume fraction (5%) of dispersed CdS nanoparticle. This indicates that only a small fraction of the chain segments that are directly attached to the CdS particles carry the effect of polymer−particle interaction in the dynamics of swelling. It is known that the spin-coated polymer films prepared at high spinning speeds remain with nonequilibrium structure. Therefore, the swelling dynamics may be affected by any residual strain that may be trapped in the films due to the large stretching at high spinning speeds. To investigate the effect of residual strain on the swelling, the film prepared with the highest spinning speed (5000 rpm), which was not preswelled, was studied in three successive dry to wet cycles. The swelling data for three repeated cycles are shown in the inset of Figure 5 (top

panel). The data in three cycles practically overlap, indicating no considerable effect of residual strain on the swelling dynamics.

4. Conclusion

In conclusion, mass uptake and swelling dynamics study of the ultrathin CdS−polyacrylamide nanocomposite spin-coated films were performed. The nanocomposite was synthesized via a chemical route and the thin films were prepared using the spin-coating technique on the silicon substrate. Both the mass uptake and the swelling dynamics of the nanocomposite films were observed to be different from those of the pure polymer films observed earlier.[1] The mass uptake of the solvent molecules in the nanocomposite films was found to obey non-Fickian behavior. The diffusion coefficient of water molecules was found to increase with the increase of the film thickness. This behavior was attributed to the thickness dependent structural changes of the nanocomposite films. The polymer−nanoparticle interaction was observed to play a significant role in governing the swelling dynamics of the nanocomposite films. A fraction of the nanocomposite system believed to be directly attached to the nanocrystalline CdS particles was found to have restricted freedom of movements due to the attractive polymer−particle interaction. The rest of the polymer chains were assumed to be relatively free during diffusion. A model in terms of the combination of the "restricted" and "free" polymer chains was proposed to account for the polymer−particle interaction in the swelling dynamics. We observe that two sets of dynamical constants independently describe the swelling dynamics of the nanocomposite films. The excluded-volume parameters were found to be about 2 orders of magnitude different for the two components of the nanocomposites, and the average diffusion coefficient for all the films corresponding to the attached fraction of polymer was found to be an order of magnitude smaller than that corresponding to the free segments as a result of the difference introduced in the structure by the nanoparticles. The observed volume fraction of the restricted component of the chains was in excellent agreement with the volume fraction of the CdS particles.

References and Notes

(1) Singh, A.; Mukherjee, M. *Macromolecules* **2003**, *36*, 8728.
(2) Vogt, B. D.; Soles, C. L.; Lee, H.-J.; Lin, E. K.; Wu, W.-l. *Langmuir* **2004**, *20*, 1453.
(3) Singh, A.; Mukherjee, M. *Phys. Rev. E* **2004**, *70*, 051608.
(4) Ouyang, J.; Chu, C.-W.; Szmanda, C. R.; Ma, L.; Yang, Y. *Nat. Mater.* **2004**, *3*, 918.
(5) Greenham, N. C.; Peng, X.; Alivisatons, A. P. *Phys. Rev. B* **1996**, *54*, 17628.
(6) Watson, A.; Wu, X.; Bruchez, M. *Biotechniques* **2003**, *34*, 269.
(7) Gao, Y.; Choudhury, N. R. *Polym. Mater. Sci. Eng.* **2001**, *84*, 986.
(8) Artemyev, M. V.; Sperling, V.; Woggon, U. *J. Appl. Phys.* **1997**, *81*, 6975.
(9) Vassiltsova, O. V.; Chuvilin, A. L.; Parmon, V. N. *J. Photochem. Photobiol. A: Chem.* **1999**, *25*, 127−134.
(10) Rama Krishna, M. V.; Friesner, R. A. *J. Chem. Phys.* **1991**, *95*, 8309.
(11) Nair, P. K.; Gomez Daza, O.; Arivas-Carbajal Readigos, A.; Campos, J.; Nair, M. T. S. *Semicond. Sci. Technol.* **2001**, *16*, 651.
(12) Willner, I.; Willner, B. *Pure Appl. Chem.* **2002**, *74*, 1773−1783.
(13) Lakowicz, J. R.; Gryczynski, I.; Grycznski, Z.; Murphy, C. J. *J. Phys. Chem. B* **1999**, *103*, 7613.
(14) Wang, Y.; Heron, N. *Phys. Rev. B* **1990**, *42*, 7253.

(15) Doi, M.; Edwards, S. F. *The Theory of Polymer Dynamics*; Clarendon Press: Oxford, 1986.

(16) Kim, D.; Caruthers, J. M.; Peppas, N. A. *Macromolecules* **1993**, *26*, 1841.

(17) Tae, G.; Kornfield, J. A.; Hubbel, J. A.; Johannsmann, D. *Langmuir* **2002**, *18*, 8241.

(18) Vrentas, J. S.; Vrentas, C. M. *J. Polym. Sci., Part B: Polym. Phys.* **1992**, *30*, 1005.

(19) VanLandigham, M. R.; Eduljee, R. F.; Gillespie, J. W. J., Jr. *Appl. Polym. Sci.* **1999**, *71*, 787.

(20) Smith, M. J.; Peppas, N. A. *Polymer* **1985**, *26*, 569.

(21) Daillant, J.; Gibaud, A. *X-Ray and Neutron Reflectivity: Principles and Applications*; Springer-Verlag: Berlin, 1999.

(22) Russell, T. P. *Materials Science Reports*; Elsevier Science Publ.: North-Holland, 1990; Vol. 5.

(23) Parratt, L. G. *Phys. Rev.* **1954**, *98*, 359.

(24) Mukherjee, M.; Deshmukh, N.; Kulkarni, S. K. *Appl. Surf. Sci.* **2003**, *218*, 323.

(25) Crank, J.; Park, G. S. *Diffusion in Polymers*; Academic Press: London, 1968.

(26) Vogt, B. D.; Soles, C. L.; Lee, H.-J.; Lin, E. K.; Wu, W.-l. *Polymer* **2005**, *46*, 1635.

(27) Shafee, E. El.; Naguib, H. F. *Polymer* **2003**, *44*, 1647.

(28) Kent, M. S.; Smith, G. S.; Baker, S. M.; Nyitray, A.; Browning, J.; Moore, G. *J. Mater. Sci.* **1996**, *31*, 927.

(29) Vogt, B. D.; Soles C. L.; Jones, R. L.; Wang, C.-Y.; Lin E. K.; Wu, W.-l.; Satija, S. K. *Langmuir* **2004**, *20*, 5285.

(30) Mukherjee, M.; Bhattacharya, M.; Sanyal, M. K.; Geue, Th.; Grenzer, J.; Pietsch, U. *Phys. Rev. E* **2002**, *66*, 061801.

(31) DeMagio, G. B.; Frieze, W. E.; Gidley, D. W.; Zhu, M.; Haristov, H. A.; Yee, A. F. *Phys. Rev. Lett.* **1996**, *78*, 1524.

(32) Pitered, E.; Bouchaud, J. P. *Eur. Phys. J. E* **2001**, *5*, 133.

(33) de Gennes, P. G. *Scaling Concepts in Polymer Physics*; Cornell University Press: Ithaca, NY, 1979.